CRITICAL FREE-SURFACE FLOW OVER A POLYGONAL OBSTACLE

Sarwat N. Hanna
Department of Engineering Mathematics and Physics, Faculty of Engineering,
Alexandria University, Alexandria Egypt.

ABSTRACT

Two-dimensional free-surface flow over a semi-infinite polygon in the bottom of an open channel is considered. The fluid is assumed to be incompressible, inviscid, and the motion is irrotational with gravity acting. A numerical method for the solution of the fully nonlinear problem is presented. For the special case of trapezoidal obstacle, critical solutions in which the flow is subcritical upstream and supercritical downstream, are obtained. The dependence of nonlinear free-surface profile on trapezoidal shape and size is discussed.

1. INTRODUCTION

This paper considers the problem of steady free-surface of a running two-dimensional, irrotational, inviscid and incompressible flow in an open channel with a nonuniform bottom in a shape of a polygon.

Far upstream the flow approaches a uniform stream with constant velocity U_1 and constant depth H_1. We define the upstream Froude number,

$$F_1 = \frac{U_1}{\sqrt{g H_1}}, \qquad (1.1)$$

where g denotes the acceleration due to gravity .

Solutions with wave downstream are not considered in this paper. Therefore, we assume that the flow approaches a uniform stream with constant velocity U_2 and constant depth H_2 far downstream and we define the downstream Froude number F_2,

$$F_2 = \frac{U_2}{\sqrt{g H_2}} . \qquad (1.2)$$

The flow is said to be subcritical when the Froude number is smaller than one and supercritical when it is greater than one.

Free-surface flows over various obstacles have been studied for at least the last century. One will find an attractive discussion of the subject in the four papers of Lord Kelvin [1]. In 1932, Lamb [2] presented a general linearized theory for flow over stream beds of arbitrary shape.

The literature of the topic is rich and in particular we may mention the work of Tuck [3], Gazdar [4], Long [5], Newmann [6] and Watters and Street [7]. Recently, a considerable amount of work has been done by Faltas, Hanna and Abd-el-Malek [8], Hanna [9],[10], Abd-el-Malek, Hanna and Kamel [11], King and Bloor [12], Forbes and Schwartz [13] and Vanden-Broeck [14].

In this paper we calculate the flow past a submerged polygonal obstacle by a series truncation procedure. This technique has been used by Birkhoff and Zarantonello [15], Dias, Keller and Vanden-Broeck [16] and Dias and Vanden-Broeck [17].

The type of solutions for which the flow is subcritical upstream and supercritical downstream is referred to as "critical flow". Critical flow is obtained by allowing the upstream Froude number F_1 to be sought as part of the solution. Such flow has been recently obtained by Naghdi and Vongsarnpigoon [19] by considering a fluid sheet over a stationary bell-shaped hump, by Forbes [18] for a submerged semicircular obstacle and by Dias and Vanden-Broeck [17] for triangular obstacles.

In this paper we solve nonlinear critical flow of ideal fluid over a polygonal obstacle numerically by specifying uniform flow upstream and downstream of the obstacle. In section (2) we formulate the problem. Solutions for polygonal obstacle are presented in

section (3). For the special case of trapezoidal obstacles solutions and results are presented and discussed in section (4).

2. FORMULATION OF THE PROBLEM

Consider a steady, two-dimensional, incompressible, and irrotational flow of an ideal fluid over a polygonal obstacle of N′ sides, placed at the bottom of an open channel Figure (1). A cartesian coordinate system is defined with origin placed horizontally at a point between 1 and N′+1, the x-axis coinciding with the stream bed before and after the obstacle and the y-axis pointing vertically upwards. Fluid flows through the channel in the positive x-direction, with speed U_1 and depth H_1 infinitely far upstream. Relative to the coordinate axis the flow is steady and is subject to the acceleration of gravity g in the negative y-direction. Suppose that the flow is critical, with unknown speed U_2 and depth H_2 far downstream, then by conservation of mass

$$Q = U_1 H_1 = U_2 H_2 \ , \qquad (2.1)$$

where Q is the discharge.

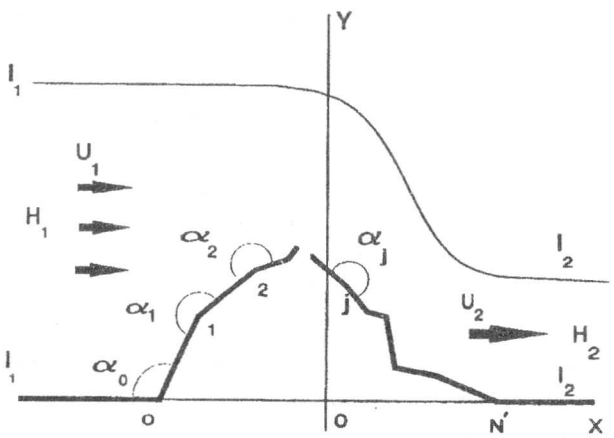

Figure 1. Sketch of the physical plane of the flow and of the coordinates and the polygonal obstacle.

Since the flow is irrotational and the fluid is incompressible, a velocity potential Φ and a stream function Ψ exist, in terms of which the horizontal and vertical components, u and v of the fluid velocity vector may be expressed as

$$u = \phi_x = \psi_y \ ; \ v = \phi_y = -\psi_x \qquad (2.2)$$

The constant pressure condition at the fluid surface leads to Bernolli's equation in the form

$$\frac{1}{2}(u^2 + v^2) + g\,y = \text{constant} \qquad (2.3)$$

on the free surface.
Evaluating (2.3) as $x \to \pm\infty$ we obtain

$$\frac{1}{2} U_1^2 + g H_1 = \frac{1}{2} U_2^2 + g H_2 \qquad (2.4)$$

This equation gives the relation,

$$(\mu - 1)[\frac{1}{2} F_2^2 (\mu + 1) - \frac{1}{\mu}] = 0, \qquad (2.5)$$

where

$$\mu = \frac{H_2}{H_1} = \frac{U_1}{U_2} \qquad (2.6)$$

Relation (2.5) shows that the two types of solutions correspond to

$$F_2^2 = \frac{2}{\mu^2 + \mu} \qquad (2.7)$$

and

$$\mu = 1 \qquad (2.8)$$

Thus for the case of critical flow $U_2 > U_1$ i.e. $\mu < 1$,it necessarily follows from (2.7) that the downstream Froude number $F_2 > 1$.

Equation (2.2) shows that the complex potential

$$\chi = \phi + i\,\psi \ , \qquad (2.9)$$

can be expressed as an analytic function of the variable

$$z = x + i\,y \ . \qquad (2.10)$$

The bottom of the channel and the obstacle are parts of

a streamline on which we require $\psi=0$. We introduce the dimensionless variables by taking $[Q^2/g]^{1/3}$ as the unit length and $[Qg]^{1/3}$ as the unit velocity. The dimensionless discharge is now equal one. Hence, the free surface is another streamline on which $\psi=1$ .In terms of the dimensionless variables, the condition (2.3) becomes

$$(\nabla\phi)^2 + 2\,y = \text{constant on } \psi = 1 \qquad (2.11)$$

The complex potential χ maps the flow domain conformably onto an infinite strip of height one as shown in Figure (2). We map this infinite strip onto the upper half of the unit disk with I_1 and I_2 corresponding to the points -1 and 1, respectively (Figure (3)), so that the solid boundary goes onto the real diameter and the free surface onto the upper half-unit circle. The images of the points $0,1,2,\ldots,N'+1$ are $t_0,t_1,t_2,\ldots,t_{N'+1}$ respectively. The map is given by

$$\chi = \frac{2}{\pi} \ln \frac{1+t}{1-t} \; ; \; |t| \le 1 \qquad (2.12)$$

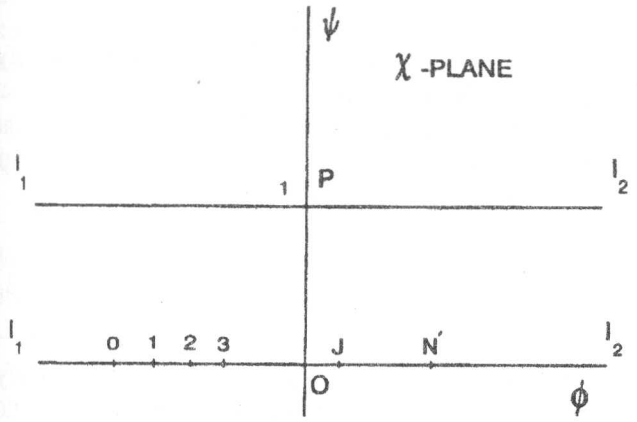

Figure 2. The complex potential plane.

The problem is now to find an analytic function z(t) satisfying the boundary condition (2.11) and mapping the streamline $\psi=0$ into the channel bottom and the obstacle. By introducing the complex conjugate velocity

$$\xi(z) = \frac{d\chi(z)}{dz} = u - iv \; , \qquad (2.13)$$

the problem becomes that of finding ξ as an analytic function of t satisfying,

$$|\xi|^2 + 2\,y = \text{constant on } |t| = 1 \qquad (2.14)$$

and the boundary condition on the real diameter $-1 \le t \le 1$.

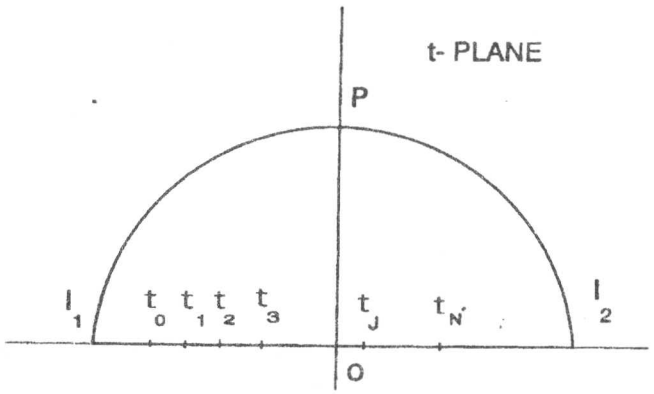

Figure 3. The complex t-plane.

3. SOLUTION

The first step is to introduce in the complex velocity the strong singularities which occur at the angled corners of the polygon at the points,

$$t = t_j \qquad j=0,1,2,..,t_{N'+1} \qquad (3.1)$$

where N′ is the number of sides of the polygon. The appropriate singularities are

$$\xi \sim (t-t_j)^{1-\frac{\alpha_j}{\pi}} \text{ as } t \to t_j \quad j=0,1,2,\ldots,N'+1 \qquad (3.2)$$

where the angles α_j satisfy the relation

$$\sum_{0}^{N'+1} \alpha_j = (N'+1)\,\pi \qquad (3.3)$$

As $\phi \to \infty$, the flow approaches a uniform supercritical stream. We introduce the angles $\alpha'_j = \alpha_j/\pi$ and we proceed to drop the primes. Therefore asymptotic form of ξ as $\phi \to \infty$ is obtained by linearizing the equations around a uniform stream [2]. This leads to,

$$\xi \sim \xi(1) + A' e^{-\lambda\chi} \quad \text{as } \phi \to \infty \qquad (3.4)$$

where A′ is a constant and λ is the smallest positive root of the equation,

$$F_2^2\lambda - \tan\lambda = 0 \qquad (3.5)$$

We rewrite the equation (3.4) in terms of t in the form,

$$\xi \sim \xi(1) + A(1-t)^{2\lambda/\pi} \text{ as } t \to \infty \qquad (3.6)$$

We now define the function $\Gamma(t)$ by the relation

$$\xi = \prod_{j=0}^{j=N'+1} \left[\frac{t-t_j}{1-t_j}\right]^{1-\alpha_j} e^{A(1-t)^{\frac{2\lambda}{\pi}} + \Gamma(t)} \qquad (3.7)$$

The function $\Gamma(t)$ is analytic for $|t| < 1$ and continuous for $|t| \leq 1$ [15]. The kinematic boundary conditions on the channel bottom and on the obstacle imply that the expansion of $\Gamma(t)$ in powers of t has real coefficients. Therefore, we can write

$$\Gamma(t) = \sum_{k=0}^{\infty} a_k t^k \qquad (3.8)$$

The unknown real coefficients a_k and A must be determined to make (3.7) satisfy the dynamic free-surface condition (2.14).

We use the relation $t = |t| e^{i\sigma}$, so that points on the free surface are given by $t = e^{i\sigma}$, $0 < \sigma < \pi$ Using (2.12) and the identity

$$\frac{\partial x}{\partial \phi} + i \frac{\partial y}{\partial \phi} = \frac{1}{\xi} \qquad (3.9)$$

We obtain after some algebra,

$$\frac{dy}{d\sigma} = -\frac{2}{\pi} \frac{v}{u^2+v^2} \frac{1}{\sin\sigma} \qquad (3.10)$$

By differentiating (2.14) with respect to σ and using (3.10) we obtain,

$$[u(\sigma)u_\sigma(\sigma) + v(\sigma)v_\sigma(\sigma)] - \frac{2}{\pi} \frac{v(\sigma)}{[u(\sigma)]^2 + [v(\sigma)]^2} \frac{1}{\sin\sigma} = 0 \qquad (3.11)$$

We now set $t = e^{i\sigma}$ in (3.7) to get $\xi(\sigma)$, and substitute the expression in (3.10). The resulting equation shall be used to determine the coefficient a_k. The next step is to express x and y as functions of ξ . Inverting (2.13) yields $\frac{dz}{d\chi} = \frac{1}{\xi}$ and thus,

$$\frac{dz}{dt} = \frac{1}{\xi} \frac{d\chi}{dt} \qquad (3.12)$$

Now by integrating (2.12) along the unit circle, we obtain

$$z(\sigma) - z_p = -\frac{2}{\pi} \int_{\frac{\pi}{2}}^{\sigma} \frac{1}{\xi(s)\sin s} ds, 0 < \sigma < \pi \qquad (3.13)$$

We solve for the a_k's numerically by truncation the infinite series in (3.8) after N term, where,

$$N = n - \left(\frac{N'}{2} + b\right) \qquad (3.14)$$

where b=4 for N'even and b=3.5 for N' odd.
We fix the geometry of the polygon by specifying $\alpha_j, j=0$ to $N'+1$ and $t_0, t_2, .., t_{N'-1}, t_{N'+1}$ for N' even and $t_0, t_2, \ldots, t_{N'}, t_{N'+1}$ for N' odd. We find the n unknowns $t_1, t_3, t_5, \ldots, \lambda, F_2, a_0, a_1, \ldots, a_N$ by collocation. Thus we introduce the n-3 mesh points,

$$\sigma_M = \frac{\pi}{(n-3)}\left(M - \frac{1}{2}\right), M=1,2,\ldots,n-3 \qquad (3.15)$$

which are substituted in (3.11) in order to satisfy it. This leads to n-3 nonlinear algebraic equations. Relation (3.5) provides another equation. By relating F_2 to the velocity downstream and rewriting (2.7) in terms of ξ, we get the required two equations

$$F_2^2 = |\xi(1)|^3 \qquad (3.16)$$

and

$$F_2^2 = \frac{2|\xi(1)|^2}{\xi(-1)[|\xi(1)| + |\xi(-1)|]} \qquad (3.17)$$

This system of n nonlinear equations with n unknowns could be solved by Newton's method.

4.APPLICATION, SUMMARY AND DISCUSSION.

Let us consider here the steady flow over semi-infinite trapezoidal obstacle consisting of a raising up inclined plane (01) at inclination angle α, horizontal plane (12) with length L and at height W from the base of the bottom, stepping down plane (23) at inclination angle $(\pi-\beta)$ as shown in Figure (4).

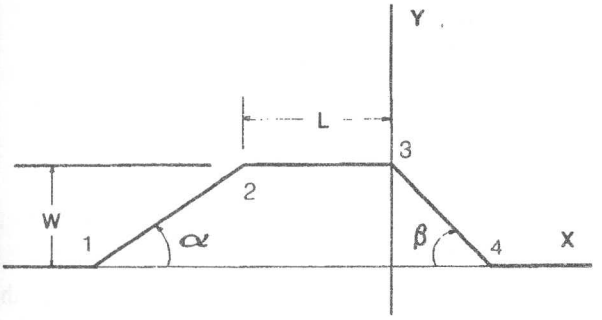

Figure 4. Shape of bottom profile in the special case of trapezoidal obstacle.

We introduce the cartesian coordinates with x-axis along the bottom and the y-axis going through the corner 2 of the trapezoidal obstacle. In this case N'=3 and equation (3.7) takes the form,

$$\xi(t)=\{\frac{t-t_0}{1-t_0}\}^{\alpha}\{\frac{t-t_1}{1-t_1}\}^{-\alpha}t^{-\beta}\{\frac{t-t_3}{1-t_3}\}^{\beta}e^{A(1-t)^{\frac{2\lambda}{\pi}}+\Gamma(t)} \quad (4.1)$$

We set $t=e^{i\sigma}$ in (4.1) and substitute ξ in (3.11). We shall use the resulting equation to determine the N coefficients a_k, where N is given by,

$$N=n-5 \quad (4.2)$$

To do so we introduce the (n-3) mesh points according to equation (3.15) and satisfy (3.11) at these points. This leads to (n-3) nonlinear algebraic equations. The relation (3.5), (3.16), and (3.17) provide the other three equations we need. We fix the geometry of the trapezoidal obstacle by specifying the angles α and β, t_0,t_3. The n unknowns are then $t_1,\lambda,F_2,A,a_0,a_1,..,a_{n-5}$. This system of n nonlinear equations with n unknowns is solved by Newton's method and Gaussian elimination method with scaled column pivoting algorithm.

Once we solve this system we calculate the height W of the obstacle by using numerical integration along the real axis of the relation (3.12).

$$W=\sin\alpha\int_{t_0}^{t_1}\{\frac{d\chi}{dt}\}\frac{1}{\xi}dt \quad (4.3)$$

We check the results by integrating the same relation between $t_2=0$ and t_3 to give the same W

$$W=\sin\beta\int_{0}^{t_3}\{\frac{d\chi}{dt}\}\frac{1}{\xi}dt \quad (4.4)$$

In order to calculate the profile we first calculate the coordinates of the point P on the free surface and with $\phi_P=0$. To do so we integrate (3.12) along the imaginary axis in t-plane between $t_2=0$ to t=i,

$$z_p=z_2+\int_{0}^{i}\frac{d\chi}{dt}\frac{1}{\xi}dt \quad (4.5)$$

where, $z_2=iW$.

Next we calculate the coordinate of the points of the free surface profile by using(3.13) in which we integrate along the unit circle in the t-plane between the point P($\sigma=\pi/2$) and the point (x,y) on the free surface.

To evaluate the upstream Froude Number F_1 we use the formula

$$F_1^2=|\xi(\pi)|^3 \quad (4.7)$$

The coefficient a_k were found to decrease rapidly as the index k increases. In table (1) we give the value of a_0 and the last coefficient a_N for values of N=5 to 25 in steps of 10 for small obstacle and for N=5 to 35 in steps of 10 for large obstacle.

Table 1. Values of a_0 and a_N for small obstacle L=0.06 and W=0.05.

N	5	15	25
a_0	-9.9268×10^{-2}	-9.9181×10^{-2}	-9.9152×10^{-2}
a_N	3.4996×10^{-6}	-6.2053×10^{-7}	-9.1021×10^{-8}

Table 2. Values of a_0,and a_N for large obstacle L=0.250 and W=0.583

N	5	15	25	35
a_0	-0.42215	-0.42203	-0.42218	-0.42223
a_N	-2.411×10^{-3}	7.027×10^{-5}	5.327×10^{-6}	6.882×10^{-7}

The profiles for different values of N for small obstacle are shown in Figure (5). The error decreases rapidly with increasing N and for N=5 its maximum value lies within 2.5×10^{-3}. Most of the computations were performed with N=35. We solved the equations with relative error smaller than 10^{-4} and we performed the integrations with an accuracy of 10^{-5}.

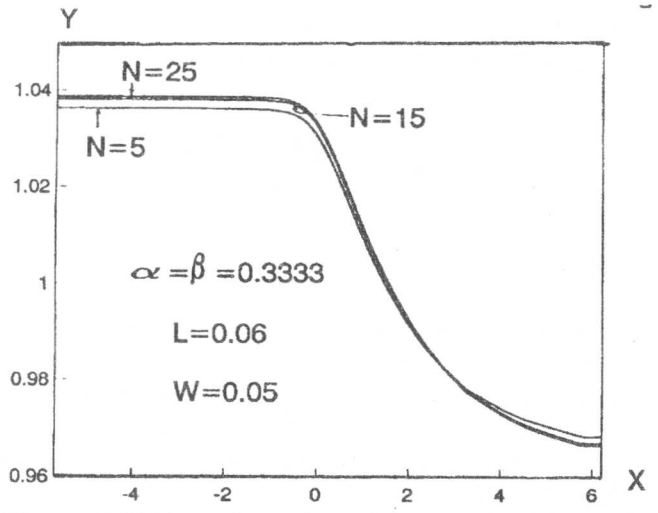

Figure 5. Effect of number of terms N of the series $\Gamma(t)$ on the free-surface profile.

4.1 *The effect of the height W on the shape of free surface profile and flow parameters*

The change of the shape of the free surface profile is shown in Figure (6) for small W and in Figure (7) for large values of W, keeping the angles α,β and the length L constant and the discharge Q=1. The upstream depth H_1 is nearly linear dependent on the height W. Downstream, the depth H_2 is also nearly linear dependent on height of the obstacle.The variation with W of the upstream Froude number F_1 and the downstream Froude number F_2 are shown in Figure (8-a) and (b) respectively. For very small W, the overall flow is nearly uniform, at the critical Froude numbers, $F_1 \to 1$ and $F_2 \to 1$ as $W \to 0$. As W is increased, F_1 decreases with W ,fast for small W and slowly for large W. The downstream Froude number F_2 increases with increasing W. Our results here are qualitatively similar to those of Forbes [18] and Naghdi and Vongsarnpigoon [19].

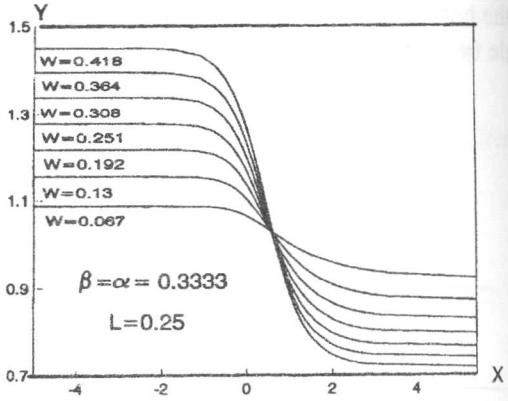

Figure 6. Effect of the height W of the obstacle, for small W, on the free-surface profiles.

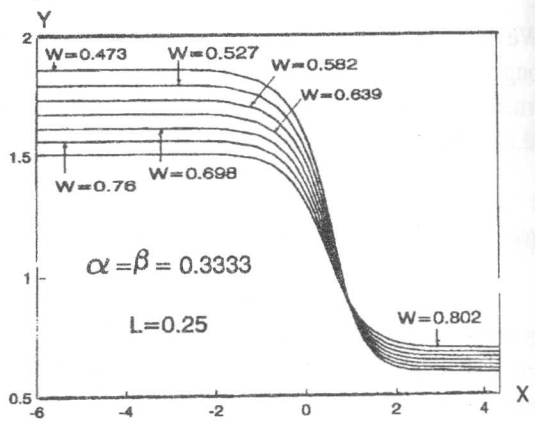

Figure 7. Effect of the height W of the obstacle, for large W, on the free-surface profiles.

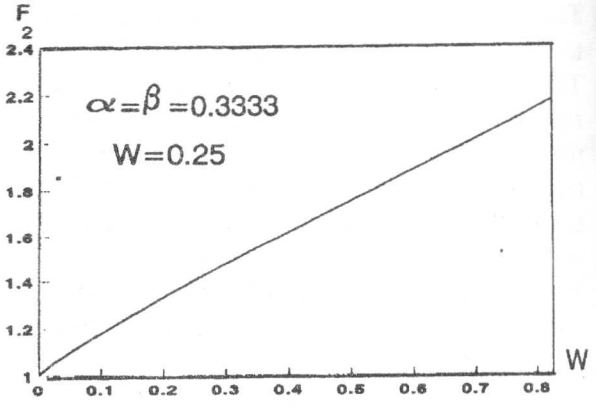

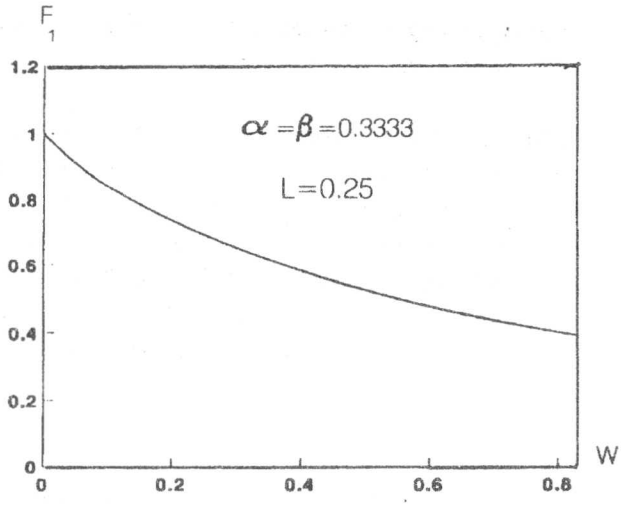

Figure 8. Effect of the height W of the obstacle on the Froude number,
(a) downstream, (b) upstream.

4.2 *The effect of inclination angle α on the shape of the free surface profile and flow parameters*

The shape of free-surface profiles for different angles α are shown in Figure (9). The increase of α influence both H_1 and H_2, weakly for large α and strongly for small α. As α is increased H_1 increases and H_2 decreases. The variation of F_2 and F_1 with the angle α is shown in Figure (10-a) and (b). F_2 drop very fast as $\alpha \to 0$ and very slow as $\alpha \to 0.5$. F_1 increases fast for small α and then slowly as α approaches 0.5.

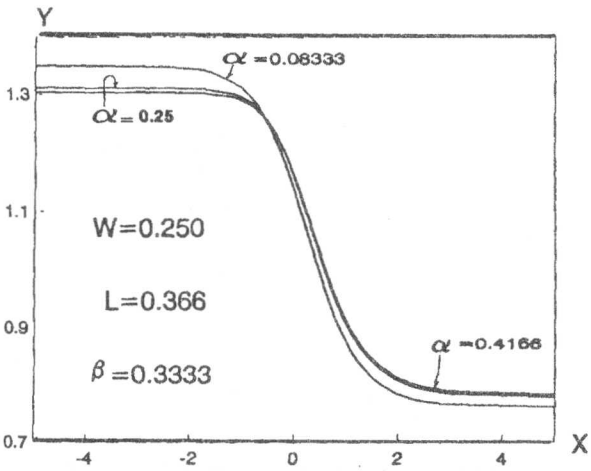

Figure 9. Effect of inclination angle α of the obstacle on the free-surface profiles.

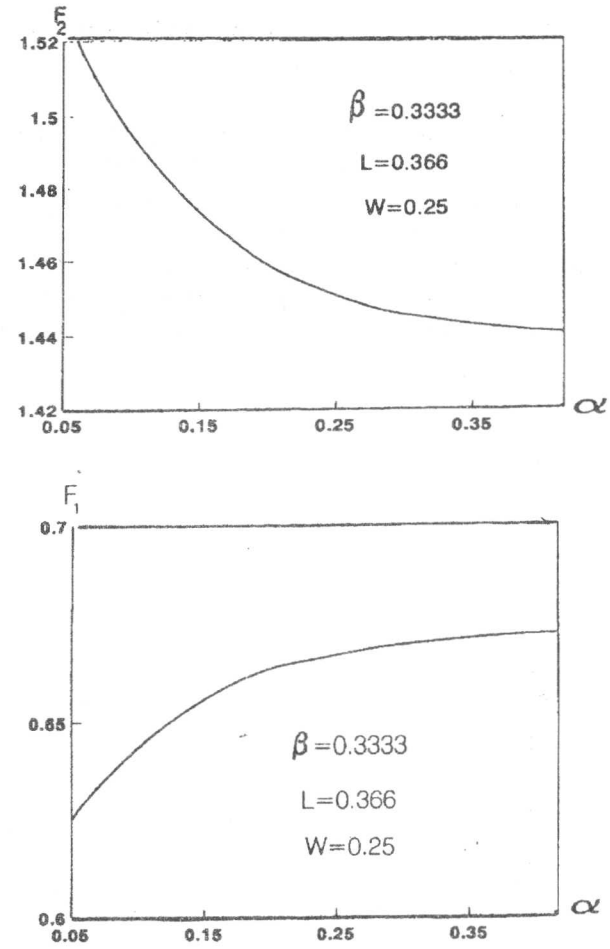

Figure 10. Effect of the inclination angle α on the Froude numbers, (a) downstream, (b) upstream.

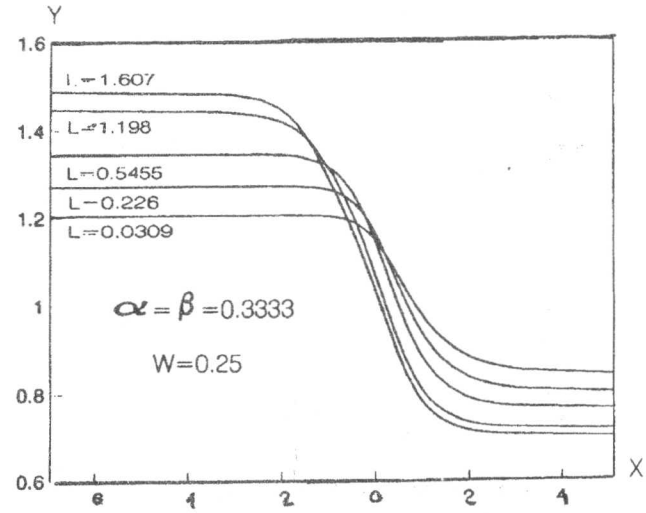

Figure 11. Effect of the top length L of the obstacle on the free-surface profiles.

4.3 *Effect of L on the shape of free-surface profile and flow parameters*

The computed free-surface profiles are displayed in Figure (11) when L varies from 0.0309 to 1.607. The depth H_1 increases and H_2 decreases with the increase of L. The depths H_1 and H_2 are very sensitive for small changes of L, for small L. On the contrary, for large L, H_1 and H_2 varied slightly for changes in L. Plots for F_2 and F_1 against L are shown in Figure (12-a) and (b).

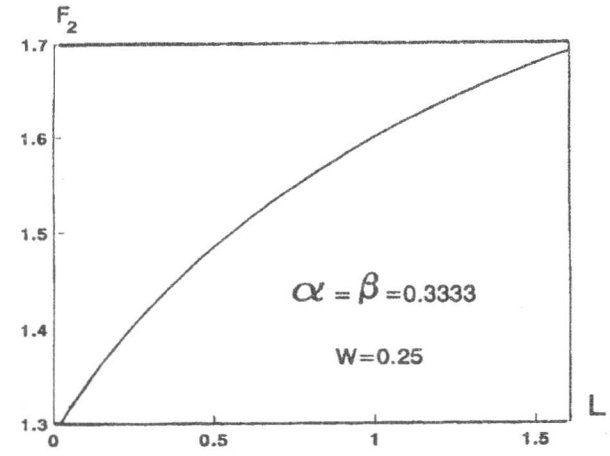

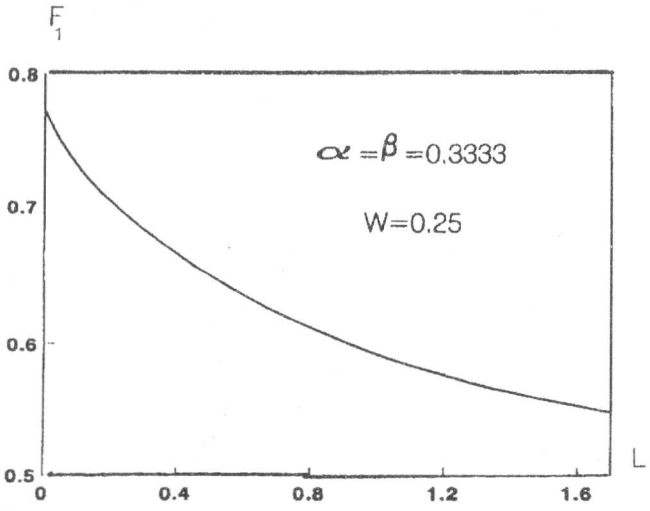

Figure 12. Effect of the top length L of the obstacle on the Froude numbers,
(a) downstream, (b) upstream.

4.4 *Effect of the inclination angle β on the shape of free-surface profile and flow parameters*

The computed free-surface profiles are displayed in Figure (13) for different values of the angle β. The depth H1 increases slightly with increasing β. The depth H_2 increases with the increase of β .It is weakly dependent on β for small β and strongly dependent on β for large β. The variation of Froude numbers upstream and downstream with the angle β are shown in Figures (14-a) and (b).

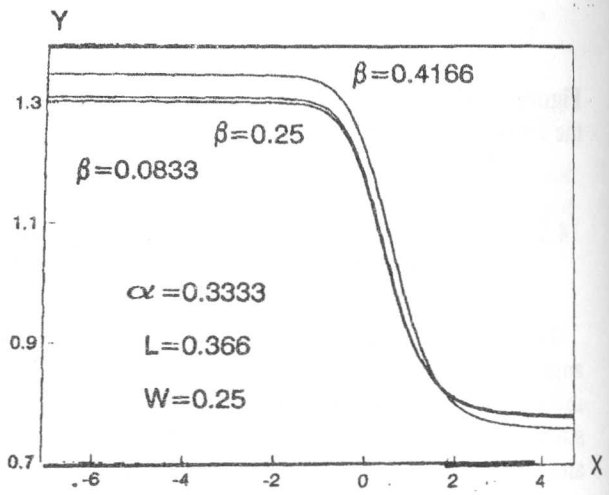

Figure 13. Effect of the descending inclination angle β on the free-surface profiles.

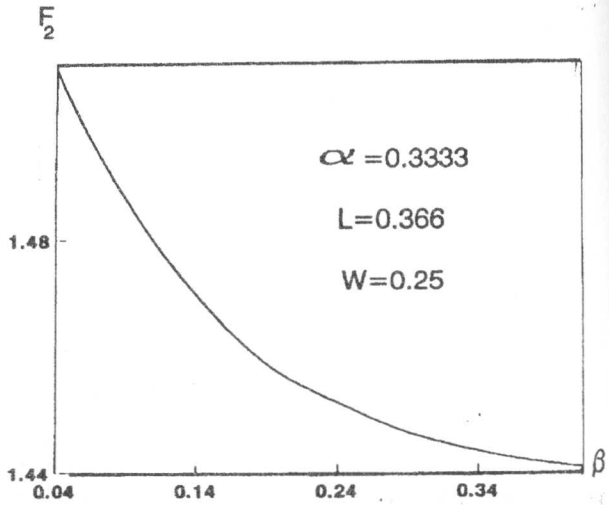

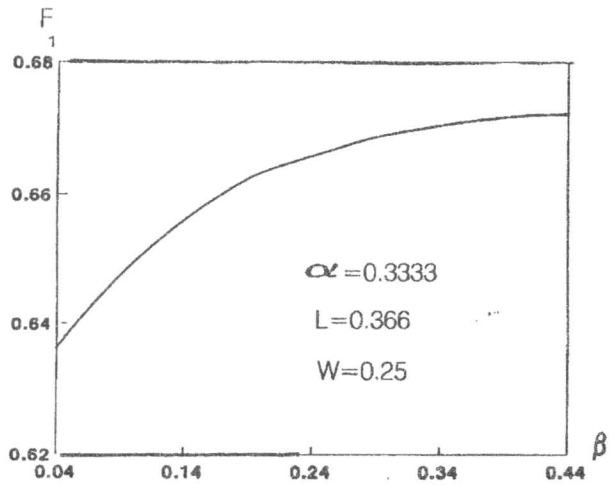

Figure 14. Effect of the descending inclination angle β on the Froude numbers,
(a) downstream, (b) upstream.

In this work the numerical algorithm of section (3) has been used to generate critical flow solutions for a variety of shapes of trapezoidal obstacle.

As a check on the numerical accuracy of our solutions, two standard internal consistency checks have been used. The first is to establish that the results are sensibly independent of the number N and the second is the computation of the height of the obstacle W in two different ways.

The computed nonlinear free-surface profiles are shown in Figures. (6), (7), (9), (11) and (12) for variations of the obstacle parameters W,α,L and β. For small obstacle there is a region of moderate curvature of the surface near the obstacle, followed by a downstream region of uniform flow having slightly reduced depth. As the obstacle becomes larger the surface slope becomes large near the obstacle, which is followed by shallow uniform stream moving at high speed.

In Figures (8), (10), (12) and (14) we present values of Froude numbers versus the different parameters of the obstacle. The Froude numbers are very sensitive to changes in W and less sensitive to changes of the parameter L and weakly dependent on the angles β and α. As the obstacle becomes larger, the downstream Froude number increases and in the limit as $W \to \infty$ the $F_2 \to \infty$ and $F_1 \to 0$.

REFERENCES

[1] Kelvin, W., "On stationary waves in flowing water", *Phil. Mag.*, **22**,353,454 (1886), **23**,52 (1887).

[2] Lamb, H., *Hydrodynamics*, 4th ed. London; Cambridge Univ. Press (1932).

[3] Tuck, E.O., "Shallow-water flows past slender bodies", *J. Fluid Mech.*, **26**(1),81-95 (1966).

[4] Gazdar, A.S., "Generation of waves of small amplitude by an obstacle on the bottom of running stream", *J. Phys. Soc. Japan*, **34**, 530-538 (1973)

[5] Long, R.R., "Blocking effects in flow over obstacles", *Tellus*, **22**, 471-480 (1970).

[6] Newman, J.N., "Propagation of water waves past long two-dimensional obstacles", *J. Fluid Mech.*, **23**, 23-29 (1965).

[7] Watters, G.Z., Street, R.L., "Two-dimensional flow over sills in open channels" *J. Hydraulic Div., ASCE.*, **90** (HY4), 107-140 (1964).

[8] Faltas M.S., Hanna S.N. and Abd-el-Malek M. B., "Linearised solution of a free-surface flow over trapezoidal obstacle", *Acta Mechanica*, **78**, 219-233 (1989).

[9] Hanna S.N., "Free-surface flow over a polygonal and smooth topography", *Acta Mech.*, to appear.

[10] Hanna S.N., "Influence of surface tension on free-surface Flow over a polygonal and curved obstruction", *J. Computational and Applied Mathematics*, to appear.

[11] Abd-el-Malek M.B., Hanna S. N.and Kamel M.T., "Approximate solution of gravity flow from a uniform channel over triangular bottom for large Froude number", *Appl. Math. Modelling*, **15**, 25-52 (1991).

[12] King A.C. and Bloor M.I.G., "Free streamline flow over curved topography", *Q. Appl. Math.*, XLVIII **2**, 281-293 (1990).

[13] Forbes L.K. and Schwartz L.W., "Free-surface flow over semicircular obstruction", *J. Fluid Mech.*, **114**, 299-314 (1982).

[14] Vanden-Broeck J., "Free-surface flow over an obstruction in a channel", *Phys. Fluid*, **30** (8) (1987).

[15] Birkhoff G. and Zarantonello, E.H., *Jets, wakes and cavities*, New York, Academic Press

(1957).

[16] Dias F., Keller J.B. and Vanden Broeck J., "Flows over rectangular wears", *Phys. Fluids*, **31**, 8 (1988).

[17] Dias F. and Vanden-Broeck J., *Open channel flows with submerged obstructions*, *J. Fluid Mech.*, **206**, 155-179 (1989).

[18] Forbes, L.K., "Critical free-surface flow over semi-circular obstruction", *J. Engng Maths.*, **22**, 3-13 (1988).

[19] Naghdi, P.M. and Vongsarnpigoon, L., "The downstream flow beyond an obstacle", *J. Fluid Mech.*, **162**, 223-236 (1986).